TITLE:

Flow boiling heat transfer of ammonia/water mixture in a plate heat exchanger

AUTHORS:

Francisco Táboas, Manel Vallès, Mahmoud Bourouis*, Alberto Coronas

CREVER – Universitat Rovira i Virgili

Av. Països Catalans No. 26, 43007 Tarragona, Spain

* Corresponding author. Tel.: +34 977558613; fax: +34 977559691; E-mail address: mahmoud.bourouis@urv.cat

ABSTRACT

The objective of this work is to contribute to the development of plate heat exchangers as desorbers for ammonia/water absorption refrigeration machines driven by waste heat or solar energy. In this study, saturated flow boiling heat transfer and the associated frictional pressure drop of ammonia/water mixture flowing in a vertical plate heat exchanger is experimentally investigated.

Experimental data is presented to show the effects of heat flux between 20 and 50 $kW \cdot m^{-2}$, mass flux between 70 and 140 $kg \cdot m^{-2} \cdot s^{-1}$, mean vapour quality from 0.0 to 0.22 and pressure between 7 and 15 bar, for ammonia concentration between 0.42 to 0.62. The results show that for the selected operating conditions, the boiling heat transfer coefficient is highly dependent on the mass flux, whereas the influence of heat flux and pressure are negligible mainly at higher vapour qualities. The pressure drop increases with increasing mass flux and quality. However, the pressure drop is independent of the imposed heat flux.

Keywords: Absorption cooling system; Experimentation; Ammonia-water; Desorption; Boiling heat transfer coefficient

NOMENCLATURE

A	heat transfer area, m^2
Cp	heat capacity, $J \cdot kg^{-1} \cdot K^{-1}$
D_h	reference hydraulic diameter, m
f	friction factor
G	mass flux $kg \cdot m^{-2} \cdot s^{-1}$
g	gravity acceleration, $m \cdot s^{-2}$
h	heat transfer coefficient, $W \cdot m^{-2} \cdot K^{-1}$
i	solution enthalpy, J/kg
L	channel length, m
m	mass flow rate, $kg \cdot s^{-1}$
Nu	Nusselt number, $Nu = \alpha D_h/\lambda$, dimensionless
P	pressure, Pa
p_r	reduced pressure, $p \cdot p_c^{-1}$
q"	heat flux, $J \cdot m^{-2} \cdot s^{-1}$
Q	heat transfer rate, W
Re	Reynolds number, $Re=GD_h/\mu$, dimensionless
Pr	Prandtl number, $Pr=cp\mu/\lambda$, dimensionless
t	width of the plate, m
U	overall heat transfer coefficient, $W \cdot m^{-2}\ K^{-1}$
x	vapor quality

Greek Letters

β_l liquid mass transfer coefficient, $m \cdot s^{-1}$

$\Delta\iota$ enthalpy increment, J/kg

ΔT temperature difference, K

ΔT_{lm} log mean temperature difference, K

ΔP pressure drop, Pa

Δx quality change

λ Stainless steel conductivity, $W \cdot m^{-1} \cdot K^{-1}$

ρ density, $kg \cdot m^{-3}$

Subscripts

calc calculated

exp experimental

eq equilibrium

f friction

l liquid phase

m average value for the two-phase mixture or between the inlet and outlet

man the test section inlet and exit manifolds and ports

mom momentum

s solution

sat	saturation
ss	solution side
sta	static
tp	two-phase
v	vapour phase
w	water
ws	water side

1 INTRODUCTION

Higher living and working standards have brought about a significant increase in the demand for air conditioning in buildings, which in turn leads to a significant increase in the demand for primary energy. Electric air conditioning systems produce peak loads on hot summer days and in recent years electric networks have barely been able to meet the demand. The fact that peak cooling demand in summer is associated with high solar radiation offers an excellent opportunity to exploit solar thermal technologies that can match heat-driven cooling technologies. Solar absorption stands out as an interesting technology to reduce electric demand and to increase the contribution of solar energy to the heating demand in winter.

Traditionally, the market for absorption refrigeration using ammonia/water has been limited to industrial plants with capacities of over 500 kW and small-capacity direct-fired machines, using natural gas as fuel, for air conditioning in the residential and commercial sector. However, there has recently been a growing demand for small-capacity machines that are thermally activated at temperatures between 80 and 120 ºC by means of waste heat or solar energy. Small-capacity systems imply additional design constraints (air-cooled systems, compactness, etc.) that can only be solved with advanced components with high performance heat and mass transfer processes.

The two main components of an absorption cycle are the absorber and the desorber. The absorption and desorption processes of the wide boiling range ammonia/water mixture are mainly governed by mass transfer rates. Therefore, it is necessary to determine the most effective geometry for enhancing the heat transfer process and especially the mass transfer process. Several researchers (Kang et al., 1998; Lee et al., 2002) have recommended plate heat exchangers for the main components of ammonia/water absorption systems in order to enhance heat and mass transfer processes, but the studies have focused on the absorber performance. As far as we know, only Roriz et al. (2004) have studied the use of a plate heat exchanger as a desorber of an ammonia/water absorption cycle. These authors have presented the first experimental results of a desorber based on a plate heat exchanger and compared the results to those obtained with a previously tested falling film desorber. They have concluded that the overall performance of the absorption machine and the heat exchanged in the desorber were similar with both types of desorbers, thereby proving the feasibility of this new kind of

compact desorber. No information has been provided by the authors about the saturated boiling heat transfer coefficient or pressure drop of the mixture.

Since the beginning of flow boiling research, flow boiling heat transfer has been recognized as the result of two contributions to the heat transfer coefficient: nucleate boiling and convective boiling. In general, the heat transfer coefficient in nucleate boiling is dependent on heat flux, while in convective boiling is mainly dependent on mass flux and vapour quality. It is still not clear from the studies published in the open literature whether the flow boiling heat transfer coefficient in plate heat exchangers is governed by nucleate or convective boiling mechanism, since both of them have been reported in literature depending on the operating conditions. Some authors concluded that the main mechanism is nucleate boiling (Panchal et al., 1983; Engelborn and Reinhart, 1990; Kumar, 1992; Pelletier, 1997; Longo and Gasparella, 2007; Palm and Claesson, 2006), whereas others only consider convective effects on the boiling coefficient (Margat et al., 1997; Han et al., 2003), and others still consider that both effects are important in the boiling process (Hsieh and Lin, 2002).

Several works have been published on plate heat exchangers in single-phase liquid-to-liquid heat transfer, but the data available on saturated boiling heat transfer are scarce. Since the advent of brazed plate heat exchangers in the 1990s, studies have focused on the boiling or evaporation of pure refrigerants or near azetropic mixtures of refrigerants for their application in refrigeration and air conditioning. In 1983, Panchal et al. (1983) investigated ammonia and R-22 flow boiling and found that heat transfer was governed by nucleate boiling for a large region of the boiling curve. Engelhorn and Reinhart (1990), using R-22 refrigerant, measured heat transfer coefficients during evaporation in a plate heat exchanger. They found that boiling heat transfer showed a strong dependence on heat flux and concluded that experimental results could be explained much better if nucleate boiling was considered. Kumar (1992) also found that the heat transfer coefficient is independent of mass flux. Pelletier and Palm (1997) arrived at the same conclusions studying the evaporation of hydrocarbons in this type of heat exchanger with the aim to use it in domestic heat pumps. Claesson (2004) studied saturated flow boiling of R-22 and R-134a in a plate heat exchanger and found that the heat transfer coefficient was best predicted by a nucleate pool boiling correlation. Longo and Gasparella (2007) reported experimental data of vaporisation heat transfer and pressure drop of three HFCs (R-134a, R-410a and R-235fa) in a PHE. The effects

of heat flux, refrigerant mass flux, saturation pressure, outlet conditions and fluid properties were investigated. The authors concluded that the heat transfer coefficient showed great sensitivity to heat flux and outlet conditions and weak sensitivity to saturation temperature but they did not clarify the mass flux effect.

A research group from China recently published three works (Yan and Lin, 1999; Hsieh and Lin, 2002 and 2003) on flow boiling conditions in a single channel of a plate heat exchanger formed by three commercial plates with a corrugation angle of 60° from the vertical axis. In the first paper, Yan and Lin (1999) studied R-134a in saturated flow boiling conditions. In this study, the authors concluded that only at high vapour qualities (>0.45) mass flux exhibits significant effects on the heat transfer coefficient. Contrary to the mass flux effects, heat flux did not show significant effects on the heat transfer at high vapour qualities, but at low qualities, with high heat fluxes, the heat transfer coefficient was influenced by the heat flux. Hsieh and Lin (2002, 2003) used the same experimental device as Yan and Lin (1999) to study the evaporation of R-410A refrigerant. In the first paper, the authors showed the heat flux effect on the saturated boiling coefficient, and in the second they showed the effect of mass flux and vapour quality. The authors concluded (Hsieh and Lin, 2003) that the heat transfer coefficient increases with the refrigerant mass flux and vapour quality even at high heat flux.

Han et al. (2003) reported experiments on the evaporative heat transfer in brazed plate heat exchangers with R-410A and R-22 refrigerants. Plate heat exchangers with different chevron angles of 45°, 35°, and 20° were used. The authors found that the heat transfer coefficient increases with increasing mass flux and vapour quality and with decreasing evaporation temperature and chevron angle. The authors therefore suggested that convective boiling was the main boiling mechanism.

Regarding all these experimental studies, it seems that those that have identified convective effects are associated with experiments carried out at high mass fluxes, typical in plate heat exchangers working as flooded evaporators, while the experiments that have only identified nucleate boiling are associated with direct expansion evaporators, in which typical operating conditions are low mass flux, pure refrigerants or near azeotropic mixtures, and moderate heat flux (Thonon, 1995).

Thonon et al. (1997) discussed the presence of both mechanisms in compact heat exchangers, including plate heat exchangers. The authors concluded that experiments performed on several geometries of compact heat exchangers clearly show that the heat transfer coefficients could be either nucleate or convective boiling mechanisms. In order to identify the boiling mechanism, the authors proposed a criterion to establish the transition between these two basic mechanisms based on the product of the Boiling and Lockhart-Martinelli numbers. For plate heat exchangers the authors identified a transition occurring at $Bo.X > 0.15 \times 10^{-3}$.

As for saturated flow boiling heat transfer, the number of publications on experimental flow boiling pressure drop in plate heat exchangers is not extensive and very recent. The experimental works published to date (Yan and Lin, 1999; Hsieh and Lin, 2002 and 2003; Longo and Gasparella, 2007), agree that the two-phase pressure drop increases with vapour quality and that higher mass flux results in a higher pressure drop for the entire quality range. The pressure drop is reduced with an increase in system pressure because of the higher specific volume of the vapour. The calculated friction factor significantly decreases with the increase of mass flux and vapour quality but is not affected to a noticeable degree by the imposed heat flux and system pressure.

No data have been found in the open literature on flow boiling heat transfer in plate heat exchangers with wide boiling range mixtures. Wenzel (1992) presented experiments with the binary mixtures of water with acetone and isopropanol but the experimental values were obtained at subcooled boiling conditions.

The objective of the work presented here is to contribute to the technological development of brazed plate heat exchangers (BPHEs) as desorbers of ammonia/water absorption machines. For this purpose an experimental setup was constructed to measure the heat transfer coefficient and pressure drop during boiling of ammonia/water mixture inside the channel of a commercial BPHE. The saturated boiling heat transfer coefficient and the two-phase pressure drop were measured with varying mass flux, heat flux, vapour quality, pressure and mixture concentration.

2 EXPERIMENTAL SETUP

An experimental test facility was constructed to study the use of brazed plate heat exchanger as desorber of an ammonia-water absorption machine. A plate heat

exchanger provided by Alfa Laval with Chevron-H type corrugation (60 deg from the plate vertical axis) was used (Fig. 1). The main geometrical characteristics of the plate are given in Table 1. The heat exchanger was made up of four plates forming three channels. The upflow of the ammonia/water solution in the central channel was heated by the downflow of water in the two external channels.

The experimental setup shown in Fig. 2 consists of four independent loops. The main loop is the ammonia/water solution circuit. The ammonia/water mixture stored in the tank is pumped through the pre-heater where the solution is heated to provide the desired vapour quality at the inlet of the plate heat exchanger, where the ammonia/water mixture boils. At the outlet of the test section, the mixture is condensed and stored again in the tank. The solution flow rate is adjusted by regulating the pump's by-pass valve. The flow rate can be further adjusted through the inverter frequency of the pump's engine. To measure the solution mass flow rate and the solution concentration, a Coriolis flow meter was installed between the pump and the pre-heater.

The other three auxiliary loops are the pre-heater loop, the hot water test section heating loop, and the condenser loop. Water was used for the auxiliary loops. The pre-heater loop provides the desired vapour quality at the inlet of the test section through the change in water temperature. The heating loop provides the heating for the test section and allows the heat flux to be fixed, controlling the hot water temperature. The condenser loop condenses the ammonia/water mixture in order to recirculate it. This circuit also controls the operation pressure by varying the water temperature. All the auxiliary loops have a circulation pump, a flow meter and an electric resistance to adjust the water temperature. The condenser circuit also has a gasket plate heat exchanger to reject the condensation heat.

The controlled variables in the experiments were the inlet solution temperature, the test section hot water inlet temperature, and the solution condensing temperature.

Pt100 sensors were used to register the temperatures at the points shown in Fig. 2. Pressure transmitters were located at the inlet and outlet of the plate heat exchanger. A coriolis mass flow meter was used to measure the mass flow of the ammonia/water solution and a vortex flow meter was used in the heating water circuit.

The test facility provides values of the overall heat transfer coefficient, which depends on the heat transfer coefficient in the hot water side, the ammonia/water mixture boiling heat transfer coefficient, and the plate wall heat transfer resistance. Since both coefficients are unknown, a previous work has been carried out to obtain the water side heat transfer coefficient. This coefficient ($\alpha_{w,ws}$) was determined experimentally by means of separate water-to-water experiments in the same test facility, using a modified Dittus-Boelter equation combined with a least-square method. The data reduction procedure is described in the following sections.

The thermodynamic properties of the ammonia/water mixture were calculated with the procedure NH_3H_2O from the Engineering Equation Solver (EES) based on the correlations of Ibrahim and Klein (1993). The transport properties of the ammonia/water mixture were calculated with the correlations presented by Conde (2004).

3 DATA REDUCTION

3.1 Single phase heat transfer

Water-to-water experiments were carried out in order to obtain the heat transfer coefficient of the water side. The experiments were done with several heat and mass fluxes, for which the heat balances on the hot and cold water sides were established, as shown in the following equations:

$$Q_{w,ws} = m_{w,ws} Cp_{w,ws} \Delta T_{w,ws} \qquad (1)$$

$$Q_{w,ss} = m_{w,ss} Cp_{w,ss} \Delta T_{w,ss} \qquad (2)$$

The energy balance between the hot and cold water sides was found to be within five percent for all runs.

The value used for the heat flux exchanged was obtained as the average value of the terms calculated by equations (1-2):

$$Q_m = \frac{Q_{w,ws} + Q_{w,ws}}{2} \qquad (3)$$

The overall heat transfer coefficient U was calculated using Q_m, the nominal heat transfer area A and the logarithmic mean temperature difference:

$$U_{\exp} = \frac{Q_m}{A\Delta T_{lm}} \qquad (4)$$

U_{exp} was compared with the U_{calc}, using Eq. (5).

$$\left(\frac{1}{U_{calc}}\right) = \left(\frac{1}{h_{w,ss}}\right) + \left(\frac{1}{h_{w,ws}}\right) + \frac{t}{\lambda} \qquad (5)$$

Substituting the values of $h_{w,ss}$ and $h_{w,ws}$ calculated by a Dittus Boelter type equation, the parameters a, b, and c of Eqs. (6-7) were adjusted by a minimum mean square error procedure.

$$Nu_{w,ws} = a\,\mathrm{Re}^{b}\,\mathrm{Pr}^{c} \qquad (6)$$

$$Nu_{w,ss} = a\,\mathrm{Re}^{b}\,\mathrm{Pr}^{c} \qquad (7)$$

3.2 Ammonia/water saturated flow boiling

The ammonia/water solution was heated in the preheater to a prescribed vapour quality before entering the test section. The heat exchanged in the test section caused an increase in the vapour quality. The quantity of vapour generated along the test section was calculated from a heat balance on the water side (Eq. (8)).

$$Q_w = m_w Cp_w \Delta T_w \qquad (8)$$

The liquid/vapour mixture enthalpy at the test section inlet was obtained considering equilibrium conditions with the inlet temperature, pressure and the overall ammonia mass fraction. Thus, the enthalpy increment of the mixture could be obtained from Q_{ws} and $m_{s,ss}$, as shown in Eq. (9).

$$\Delta i_s = \frac{Q_{ws}}{m_{s,ss}} \qquad (9)$$

The outlet mixture enthalpy, calculated from the water side heat balance was compared with the calculated outlet enthalpy considering equilibrium conditions with the measured pressure, temperature and overall ammonia mass fraction at the test section outlet.

$$Q_s = m_s (i_{oulet,eq} - i_{inlet,eq}) \qquad (10)$$

The solution vapour quality at the inlet and outlet of the test section was calculated considering equilibrium with the temperature, pressure and enthalpy data. Only if the difference between Eq. 8 and Eq. 10 was less than 10%, the experimental data was considered valid.

The boiling heat transfer coefficient was derived from the overall heat transfer coefficient U:

$$\left(\frac{1}{h_{tp}}\right) = \left(\frac{1}{U}\right) - \left(\frac{1}{h_{w,ws}}\right) - \frac{t}{\lambda} \qquad (11)$$

where the heat transfer coefficient on the water side is determined from the single-phase water-to-water heat transfer correlation established in this study.

3.3 Frictional pressure drop

The total pressure drop of a fluid is the sum of the static pressure drop, momentum pressure drop, and that resulting from friction on the channel walls. In order to evaluate the friction factor associated with ammonia/water flow boiling in the channel of the plate heat exchanger, the frictional pressure drop $\Delta P_{f,tp}$ was calculated by subtracting the static pressure drop (elevation head) ΔP_{sta}, the momentum pressure drop (acceleration) ΔP_{mom}, and pressure losses at the inlet and outlet of the test section manifolds and ports ΔP_{man} from the total or measured pressure drop ΔP_{total}.

$$\Delta P_{f,tp} = \Delta P_{total} - \Delta P_{sta} - \Delta P_{mom} - \Delta P_{man} \qquad (12)$$

The momentum and gravity pressure drops were estimated by the homogeneous model for two-phase flow as follows:

$$\Delta P_{mom} = G^2 \left(\frac{1}{\rho_v} - \frac{1}{\rho_l} \right) \Delta x \qquad (13)$$

$$\Delta P_{sta} = g \rho_m L \qquad (14)$$

where Δx is the vapour quality change between the inlet and outlet of the channel, and

$$\rho_m = \left[\frac{x_m}{\rho_v} + \frac{(1 - x_m)}{\rho_l} \right]^{-1} \qquad (15)$$

is the average two-phase density between inlet and outlet calculated by the homogeneous model.

For plate heat exchangers (PHEs), some authors (Margat, 1997; Sterner and Sunden, 2006; Palm and Claesson, 2006) have recommended the use of a heterogeneous model to estimate acceleration and gravitational pressure drop. Based on the experimental data obtained by Margat (1997), it seems that the void fraction in a plate heat exchanger is low and a homogeneous model overpredicts the void fraction. However, most of the authors who have published experimental data on pressure drop in PHEs (Hsieh and Lin , 2002 and 2003; Longo and Gasparella, 2007; Jokar et al., 2006), have used a homogeneous model to estimate acceleration and gravitational pressure drop.

In the present experimental work, the differences between the predicted values obtained from the homogenous and heterogeneous models were less than 1000 Pa for the gravitational pressure drop and 150 Pa for the acceleration pressure drop. These values are in good agreement with the results published by Tribbe and Muller-Steinhagen (2001).

The pressure drop at the inlet and outlet manifolds and ports may be approximately calculated, according to the outline proposed by Hsieh and Lin (2002), as:

$$\Delta P_{man} \cong 1.5\left(\frac{G^2}{2\rho_m}\right) \qquad (16)$$

Once $\Delta P_{f,tp}$ is obtained, the two-phase Fanning friction factor can be determined from Eq. (17).

$$f = (\Delta P_{f,tp} D_h \rho_m)/(2G^2 L) \qquad (17)$$

3.4 Uncertainty of the measured and calculated parameters

The monitoring system used in the present work recorded temperatures, pressures and mass flow rates of both hot water and ammonia-water solution. The uncertainties of the experimental results were analysed according to the methodology described in NIST Technical Note 1297. Table 2 summarizes the most significant data. The uncertainty in the boiling heat transfer coefficient increases as the solution mass flux increases because the higher solution heat transfer coefficient reduces the difference between the overall heat transfer coefficient and the water-side heat transfer coefficient. The uncertainty associated with pressure measurements and vapour quality are the main uncertainty sources in the calculated Fanning friction factor.

4 RESULTS AND DISCUSSION

4.1 Single-phase water-to-water experiments

Several researchers have studied the single-phase heat transfer coefficient for plate heat exchangers. Most of them correlated the heat transfer coefficient using a modified

Dittus-Boelter type equation, in which the constants and exponents were changed. An exhaustive compilation of some of the most important correlations was reported by Ayub (2003) and a comparison was presented by Garcia-Cascales et al. (2007). In the present work, the single phase water-to-water results were compared to those obtained through the correlations of Wanniarachchi et al. (1995), Okada et al. (1972), Thonon (1995), Kumar (1984) and Muley and Manglik (1999).

Figure 3 compares the experimental overall heat transfer coefficient calculated by Eq. (4) with the overall heat transfer coefficient calculated by Eq. (5) using the considered correlations to evaluate the water convection heat transfer coefficients. As shown in Fig. 3, the correlations of Okada et al. (1972), Muley and Manglik (1999), and Wanniarachchi et al. (1995) give similar predictions, and slightly underpredict the experimental data. The correlation of Thonon (1995) tends to over predict the experimental data. The correlation of Kumar (1984) can predict all the experimental data obtained within 10% and was therefore selected in the present work to calculate the single-phase water-to-water coefficient.

4.2 Flow boiling heat transfer coefficient

The effects of pressure, concentration, and mass and heat fluxes on the boiling heat transfer coefficient of the ammonia/water mixture were examined using the data obtained in the experimental setup. The experiments were conducted taking into account the typical operating conditions of absorption cooling systems and the thermodynamic properties of the working fluids. The ammonia mass fraction varied between 0.33 to 0.62, mass flux between 50 and 140 $kg \cdot m^{-2} \cdot s^{-1}$, heat flux from 20 to 70 $kW \cdot m^{-2}$, and pressure from 7 bar to 15 bar. The inlet conditions were varied from subcooled conditions to 0.2 of vapour quality.

4.2.1 Mass flux effect on the boiling coefficient

Figure 4(a) shows the mass flux effect on the heat transfer coefficient for different mass fluxes between 50 and 140 $kg \cdot m^{-2} \cdot s^{-1}$, at a constant pressure of 15 bar and a heat flux of 30 $kW \cdot m^{-2}$. Different trends in the heat transfer coefficient were obtained with increased vapour quality, as shown in Fig. 4(a). For mean vapour qualities lower than 0.05, there

is a sharp increase in the boiling coefficient until it reaches a maximum point at which the boiling curve tends to stabilize. Afterwards, the influence of the vapour quality influence diminishes until it reaches a mean vapour quality of 0.1. Beyond this value the trend of the boiling coefficient depends mainly on the mass flux considered, showing a slight increase with the vapour quality at 100 and 140 $kg \cdot m^{-2} \cdot s^{-1}$ and a slight decrease at 50 and 70 $kg \cdot m^{-2} \cdot s^{-1}$.

This behaviour was reproduced with data obtained at different heat fluxes. Figures 4(b) and 4(c) show data obtained at the same conditions as Fig. 4(a), but with a heat flux of 20 $kW \cdot m^{-2}$ and 40 $kW \cdot m^{-2}$, respectively.

The sharp increase in the boiling coefficient at the lower vapour qualities might be explained by the fact that that the mixture entering the plate heat exchanger has some degree of subcooling. Figure 5 presents the same data considered for Fig. 4(a) using the vapour quality at the inlet of the plate heat exchanger at the horizontal axis. The local maximum of the boiling coefficient obtained experimentally at vapour qualities of less than 0.05 coincides with the point at which the mixture reaches the saturation state at the inlet.

Based on the trends discussed above, it is possible to consider a region in which the vapour quality does not affect the heat transfer coefficient. This could be explained by nucleation effects, although the increase of boiling coefficients leading to increased mass flux observed in this region is not typical in nucleate boiling. Hsieh and Lin (2002) also observed that even when nucleation effects are present, the mass flux influences the boiling coefficient. These authors suggested that turbulence causes the bubbles to leave the plate earlier, and then enhances bubble generation frequency. Because ammonia/water is a mixture with a wide boiling range, another explanation for this mass flux effect could be that the bubbles departing the plate earlier promotes the renewal of the mass diffusion boundary layer between the liquid and the vapour, thus reducing the mass transfer resistance. In this context, Wettermann and Steiner (2000) proposed introducing the mass flux variable to predict the parameter (B_0/β_L) of the Schlünder (1982) correlation in their study dealing with flow boiling heat transfer in tubes of wide-boiling mixtures.

4.2.2 Heat flux effect on the boiling coefficient

Figure 6 shows the effect of heat flux on the heat transfer coefficient at a constant mass flux of 100 $kg \cdot m^{-2} \cdot s^{-1}$. It can be seen that the heat flux influences the boiling heat transfer coefficient only in the low mean vapour quality region where the heat transfer coefficient slightly increases with heat flux. These experimental results are in fair agreement with those obtained by Hsieh and Lin (2003) and those of Han et al. (2003) in their work on vaporization of HFC-410a inside a BPHE. These authors also reported slight influence of the heat flux even at the lower vapour qualities, but it should be noted that these authors carried out their experiments at heat fluxes lower than 15 $kW \cdot m^2$. The suppression of nucleate boiling observed from the experimental data at very low vapour qualities, even for higher heat fluxes, is probably due to the wide boiling range of the ammonia/water mixture.

Figure 6 shows that the data series for heat flux of 20 and 30 $kW \cdot m^{-2}$ give similar boiling heat transfer coefficients; however the data for 40 and 50 $kW \cdot m^{-2}$ exhibit some dependency on heat flux, which indicates that nucleate boiling effects are present. Another interesting point is that after the sharp increase at the beginning of the boiling curve, between 0.03 and 0.07 of the mean vapour quality, the boiling heat transfer coefficient reaches its maximum point and then smoothly decreases until the point at which the heat flux effect is negligible and convective boiling effects appear. Since this behavior was not reported in other bibliographic references of boiling heat transfer in plate heat exchangers, it was assumed to be due to the mixture effects in the nucleate boiling region. Figure 6 also shows that when the mean vapour quality increases, it reaches an inflection point after which the heat transfer coefficient increases significantly with the mean vapour quality. This point indicates the beginning of convective boiling. The higher the heat flux, the higher the mean vapour quality at which convective boiling begins, which is similar to the trend observed for flow boiling in tubes. Finally, it can be seen that in the convective boiling region the boiling heat transfer coefficient becomes insensitive to heat flux and the curves follow the same trend.

4.2.3 Pressure effect on the boiling coefficient

Typically, the nucleate boiling coefficient increases when the system pressure increases and this influence is less pronounced for mixtures than for pure components because diffusion mass transfer at the liquid/vapour interface controls the boiling process. In the convective boiling region, the boiling heat transfer coefficient normally increases when the system pressure decreases because vapour density is then reduced.

To study the pressure effect on the flow boiling heat transfer coefficient, experiments were performed at typical pressures for ammonia/water absorption cooling systems. Figure 7 shows data of the boiling heat transfer coefficient achieved with pressures of 7, 10 and 15 bar, at the same heat flux of 30 $kW \cdot m^{-2} \cdot K^{-1}$ and mass flux of 70 $kg \cdot m^2\ s^{-1}$, for which it was considered that the heat transfer coefficient should be mainly controlled by nucleate boiling effects. The results indicate that the flow boiling heat transfer coefficient is not affected by the system pressure. Nevertheless, it should be noted that the pressure range considered corresponds to a reduced pressure ranging from 0.034 to 0.07, which is not enough to show a significant effect of pressure on the boiling heat transfer coefficient. The same trend was observed with data obtained at a higher mass flux of 140 $kg \cdot m^{-2} \cdot s^{-1}$ where convective boiling predominates.

4.2.4 Ammonia mass fraction effect on the boiling coefficient

Taking the operating conditions of ammonia/water absorption cooling systems into account, the ammonia mass fraction range considered in the experiments was from 0.42 to 0.62. This concentration range corresponds to a minimum of the pool boiling coefficient in the experimental data reported by Inoue et al. (2002). Hence, the nucleate boiling coefficient term is expected to be small and this could explain why the flow boiling coefficient was slightly affected by the heat flux.

Figure 8(a) shows experimental data of the boiling heat transfer coefficient obtained at a mass flux of 140 $kg \cdot m^{-2} \cdot s^{-1}$ for different mass fractions of ammonia, while Fig. 8(b) shows the corresponding data of the same parameter for a mass flux of 70 $kg \cdot m^{-2} \cdot s^{-1}$ at which convective boiling was not achieved. The results indicate that, for the mass

fraction range considered, an increase in the ammonia mass fraction results in an insignificant change in the boiling heat transfer coefficient.

4.2.5 Comparison with flow boiling experiments in tubes

Khir et al. (2005a and 2005b) published experimental data on ammonia/water flow boiling in tubes at operating conditions similar to those considered in the present work. The test section was a 6 mm diameter vertical smooth tube. To compare their data and our experiments, we selected a heat flux of 66.52 $kW \cdot m^{-2}$ and a mass flux of 70.73 $kg \cdot m^{-2} \cdot s^{-1}$ and an ammonia mass fraction of 0.55. We did not observe big differences in the data of the two geometries. However, it is important to consider that the water side heat transfer coefficient can be three times higher in a plate heat exchanger, which results in a higher overall heat transfer coefficient.

4.3 Flow boiling pressure drop

All the pressure drop terms can be calculated using the experimental values of the inlet and outlet vapour qualities, mass flux and liquid and vapour thermophysical properties. Hence, the experimental two-phase frictional pressure drop was obtained from Eq. (16) by subtracting the acceleration, gravitational and manifolds and ports pressure drops from the total measured pressure drop.

Since the vapour quality change in the channel is less than 0.2 the acceleration pressure drop term was found to be relatively small. Also, the pressure losses at the test section inlet and outlet manifolds and ports are very small compared to the total pressure drop. Only the gravitational pressure drop ranges from 1%, with a mean vapour quality of 0.2 to 13%, for a mean vapour quality of 0.04. If a homogeneous model is used, the gravitational pressure is less than 8% because of the higher void fraction obtained with this kind of model.

The variations of the frictional pressure drop in the BPHE channel with the vapour quality at different mass fluxes are shown in Fig. 9 (a). The results outline the strong effect of the vapour quality and mass flux on the pressure drop with a greater pressure drop as the vapour quality increases. Experimental results obtained by Hsieh and Lin (2003), Han et al. (2003), Longo and Gasparella (2007) agree with the results reported in this figure. Figure 9(b) illustrates the frictional pressure drop at two system pressures

of 7 and 15 bar and a mass flux of 100 $kg \cdot m^{-2} \cdot s^{-1}$. It can be observe that the frictional pressure drop is reduced when the system pressure is increased, which is mainly attributed to the fact that for a lower system pressure the vapour density is lower, thereby increasing vapour velocity.

Figure 10 shows the friction factor obtained at three mass fluxes of 70, 100 and 140 $kg \cdot m^{-2} \cdot s^{-1}$ and a heat flux of 30 $kW \cdot m^{-2}$. The results indicated that the friction factor decreases significantly from 1.4 to about 0.8 when the mean vapour quality increases up to 0.1. Above this value, we did not observe a significant effect of the mean vapour quality on the friction factor and on the mass flux.

5 CONCLUSIONS

An experimental investigation has been carried out to measure the flow boiling heat transfer coefficient and the associated frictional pressure drop for different ammonia/water mixtures under flow boiling conditions in a vertical channel of a brazed plate heat exchanger. The effects of mass flux, heat flux, pressure, and ammonia mass fraction on the flow boiling heat transfer coefficient and pressure drop were analysed at mean vapour qualities up to 0.22. The experimental conditions were selected considering the operating conditions of the ammonia/water absorption cooling systems driven by low temperature heat sources.

The following conclusions were derived from the experimental data:

1) The boiling heat transfer coefficient shows a sharp increase as the mean vapour quality increases up to 0.05, afterwards an intermediate region is observed, in which the vapour quality has a little influence and the heat transfer coefficient tends to decrease slightly, followed by a region where another increase is observed for the higher mass fluxes considered.

2) The main parameter influencing the boiling heat transfer coefficient is the mass flux. The influence of heat flux is much less pronounced and should only be considered at vapour qualities of less than 0.1. The system pressure shows a slight influence on the saturated flow boiling heat transfer coefficient. The ammonia mass fraction does not show appreciable effects in the range of 0.42 to 0.62.

3) The frictional pressure drop increases with the mass flux and almost linearly with the mean vapour quality. Nevertheless, the influence of the imposed heat flux and system pressure on the frictional pressure drop is relatively small.

ACKNOWLEDGEMENTS

The authors would like to thank Alfa Laval for providing the plate heat exchangers and the Spanish Ministry of Science and Technology for subsidizing the research project of reference: DPI2002-04536-C02-01.

REFERENCES

1. Kang, Y.T., Christensen, R.N., Kashiwagi, T., 1998. Ammonia–wate bubble absorber with a plate heat exchanger, ASHRAE Trans. 104, pp. 1-11.

2. Lee, K.B., Chung, B.H., Lee, J.C., Lee, C.H., Kim, S.H., 2002. Experimental analysis bubble mode in a plate-type absorber, Chem. Enginnering Sc., 57, pp. 1923-1929.

3. Roriz, L., Mortal, A., Mendes, L. F., 2004. Study of a plate heat exchanger desorber with a spray column for a small solar powered absorption machine. 3rd International conference on heat powered cycles, Cyprus.

4. Panchal, C. B., Hillis, D. L., Thomas, A., 1983. Convective boiling of ammonia and Freon 22 in plate heat exchangers. In ASME/JSME Thermal engineering Joint Conference.

5. Engelhorn, H. R., Reinhart, A. M., 1990. Investigations on heat transfer in a plate evaporator. Chemical Engineering Process, 28, pp. 143-146.

6. Kumar, H., 1992. The design of plate heat exchangers for refrigerants. Proceedings Institute of refrigeration.

7. Pelletier, O., Palm, B., 1997. Boiling of hidrocarbons in small plate heat exchangers. In International institute of refrigeration Commission B1, College park USA.

8. Claesson, J., 2004. Thermal and hydraulic performance of compact brazed plate heat exchangers operating as evaporators in domestic heat pumps, KTH (Royal institute of technology), Stockholm, pp. 252.

9. Longo, G.A., Gasparella, A., 2007. Heat transfer and pressure drop during HFC refrigerant vaporization inside a brazed plate heat exchanger. International Journal of Heat and Mass Transfer, 50, pp. 5194-5203

10. Yan, Y.Y., Lin, T.F., 1999. Evaporation heat transfer and pressure drop of refrigerant R-134a in a plate heat exchanger. Journal of Heat Transfer-Transactions of the ASME, 121(1), pp. 118-127.

11. Hsieh, Y.Y., Lin, T. F., 2002. Saturated flow boiling heat transfer and pressure drop of refrigerant R-410A in a vertical plate heat exchanger. International Journal of Heat and Mass Transfer, 45(5), pp. 1033-1044.

12. Hsieh, Y.Y., Lin, T. F., 2003. Evaporation heat transfer and pressure drop of refrigerant R-410A flow in a vertical plate heat exchanger. Journal of Heat Transfer-Transactions of the ASME, 125(5), pp.852-857.

13. Han, D.H., Lee, K.J., Kim, Y.H., 2003. Experiments on the characteristics of evaporation of R410A in brazed plate heat exchangers with different geometric configurations. Applied Thermal Engineering, 23(10), pp. 1209-1225.

14. Thonon, B., Feldman, A., Margat, L., Marvillet, C., 1997. Transition from nucleate boiling to convective boiling in compact heat exchangers. International Journal of Refrigeration, 20(8), pp. 592-597.

15. Wenzel, U., 1992. Saturated pool boiling and subcooled flow boiling of mixtures at atmospheric pressure. University of Auckland.

16. Ibrahim, O.M., Klein, S.A., 1993. Thermodynamic Properties of Ammonia Water mixtures. ASHRAE Transactions, 99, pp. 1495-1502.

17. Conde, M., 2004. Thermophysical Properties of {NH_3 + H_2O} Solutions for the Industrial Design of Absorption Refrigeration Equipment (Available from: http://www.mrc-eng.com/).

18. Margat, L., 1997. Étude thermohydraulique en evaporation de la charge en fluide diphasique dans un canal corrugué brasé. Université de Provence Aix-Marseille I, pp. 306.

19. Sterner, D., Sunden, B., 2006. Performance of plate heat exchangers for evaporation of ammonia. Heat Transfer Engineering, 27(5), pp. 45-55.

20. Palm, B., Claesson, J., 2006. Plate heat exchangers: Calculation methods for single-and two-phase flow. Heat Transfer Engineering, 27(4), pp. 88-98.

21. Jokar, A., Hosni, M.H., Eckels, S.J., 2006. Dimensional analysis on the evaporation and condensation of refrigerant R-134a in minichannel plate heat exchangers. Applied Thermal Engineering, 26 (17-18), pp. 2287-2300.

22. Tribbe, C., Muller-Steinhagen, H.M., 2001. Gas/liquid flow in plate-and-frame heat exchangers - Part II: Two-phase multiplier and flow pattern analysis. Heat Transfer Engineering, 22(1), pp. 12-21.

23. Ayub, Z.H., 2003. Plate heat exchanger literature survey and new heat transfer and pressure drop correlations for refrigerant evaporators. Heat Transfer Engineering, 24(5), pp.3-16.

24. García-Cascales, J.R., Vera-García, F., Corberán-Salvador, J.M., Gonzálvez-Maciá, J., 2007. Assessment of boiling and condensation heat transfer correlations in the modelling of plate heat exchangers. International Journal of Refrigeration, 30(6), pp. 1029-1041.

25. Wanniarachchi, A.S., Ratman, U., Tilton, B.E. Dutta-Roy, K., 1995. Aproximate correlations for chevron-type plate heat exchangers. In 30th National heat transfer conference. ASME, New York.

26. Okada, K., Ono, M., Tomimura, T., Okuma, T., Konno, H., Ohtani, S., 1972. Design and Heat trasnfer characteristics of a new plate heat exchanger. Heat transfer Japanese Research, 1(1), pp. 90- 95.

27. Thonon, B., 1995. Design method for plate evaporators and condensers. in 1st International conference on process Intensification for the chemical industry.

28. Kumar, H., 1984. The plate heat exchanger: Construction and Design. In Institute of chemical engineering Symposium series.

29. Muley, A., Manglik, R.M., 1999. Experimental study of turbulent flow heat transfer and pressure drop in a plate heat exchanger with chevron plates. Journal of Heat Transfer-Transactions of the ASME, 121(1), pp. 110-117.

30. Wettermann, M., Steiner, D., 2000. Flow boiling heat transfer characteristics of wide-boiling mixtures. International Journal of Thermal Sciences, 39(2), pp. 225-235.

31. Schlünder, E.U., 1982. Heat transfer in nucleate boiling of mixtures. International Chemical Engineering, 23, pp. 589-599.

32. Inoue, T., Monde, M., Teruya, Y., 2002. Pool boiling heat transfer in binary mixtures of ammonia/water. International Journal of Heat and Mass Transfer, 45(22), pp. 4409-4415.

33. Khir, T., Ben Brahim, A., Jassim, R.K., 2005a. Boiling by forced convection of water-ammonia mixtures in a vertical tube. Canadian Journal of Chemical Engineering, 83(3), pp. 466-476.

34. Khir, T., Jassim, R.K., Ghaffour, N., Ben Brahim, A., 2005b. Experimental study on forced convective boiling of ammonia-water mixtures in a vertical smooth tube. Arabian Journal for Science and Engineering, 30(1B), pp.47-63.

35. Margat, L., Thonon, B., Tadrist, L., 1997. Heat Transfer and Two Phase Flow Characteristics During Convective Boiling in a Corrugated Channel. In Compact Heat Exchangers for the Process Industry, Begell House.

6 FIGURE CAPTIONS

Figure 1. Scheme of the plate heat exchanger

Figure 2. Schematic diagram of the experimental set-up

Figure 3. Differences between the calculated and experimental overall heat transfer coefficient, in single phase experiments with water obtained by available correlations.

Figure 4. Boiling heat transfer coefficient vs. the mean vapour quality for different mass fluxes ((a): q”=30 $kW \cdot m^{-2}$, P=15 bar, w=0.42 ; (b): q”=20 $kW \cdot m^{-2}$, P=15 bar, w=0.42 ; (c): q”=40 $kW \cdot m^{-2}$, P=15 bar, w=0.42)

Figure 5. Boiling heat transfer coefficient vs. the inlet vapour quality for different mass fluxes (q”=30 $kW \cdot m^{-2}$, P=15 bar, w=0.42)

Figure 6. Boiling heat transfer coefficient vs. the mean vapour quality for different heat fluxes (G=100 $kg \cdot m^{-2} \cdot s^{-1}$, P=15 bar, w=0.42)

Figure 7. Boiling heat transfer coefficient vs. the mean vapour quality for different pressures (G=70 $kg \cdot m^{-2} \cdot s^{-1}$, q”=30 $kW \cdot m^{-2}$, w=0.42)

Figure 8. Boiling heat transfer coefficient vs.the mean vapour quality for different ammonia mass fractions (q”=30 $kW \cdot m^{-2}$, P=15 bar, (a): G=140 $kg \cdot m^{-2} \cdot s^{-1}$ and (b): G=70 $kg \cdot m^{-2} \cdot s^{-1}$)

Figure 9. Pressure drop vs. the mean vapour quality ((a): mass flux effect, (b): pressure effect).

Figure 10. Friction factor vs. the mean vapour quality at different mass fluxes.

7 TABLE CAPTIONS

Table 1. Specifications of the plate heat exchanger

Table 2. Summary of the uncertainty analysis

Figure 1

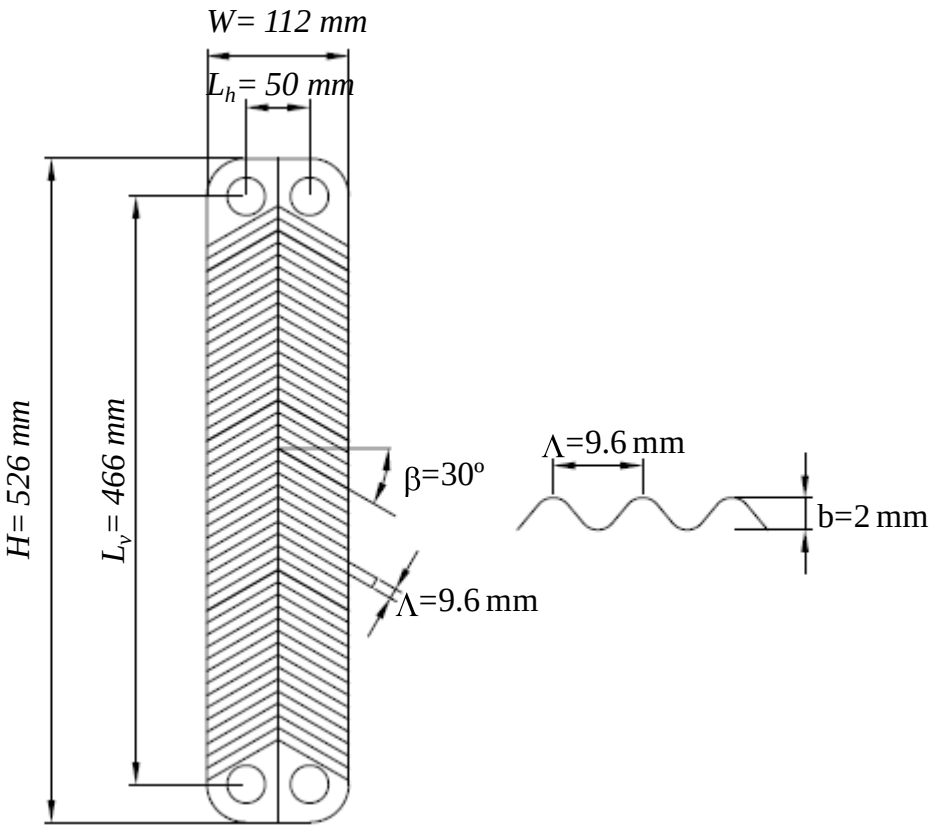

Figure 1. Scheme of the plate heat exchanger

Figure 2

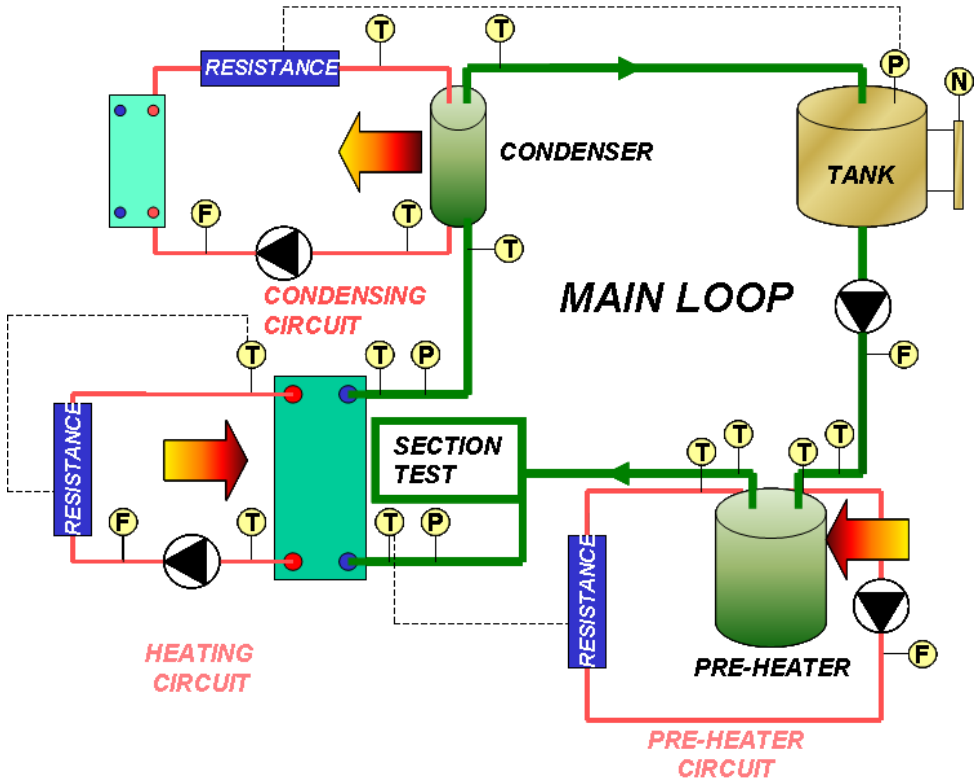

Figure 2. Schematic diagram of the experimental set-up

Figure 3

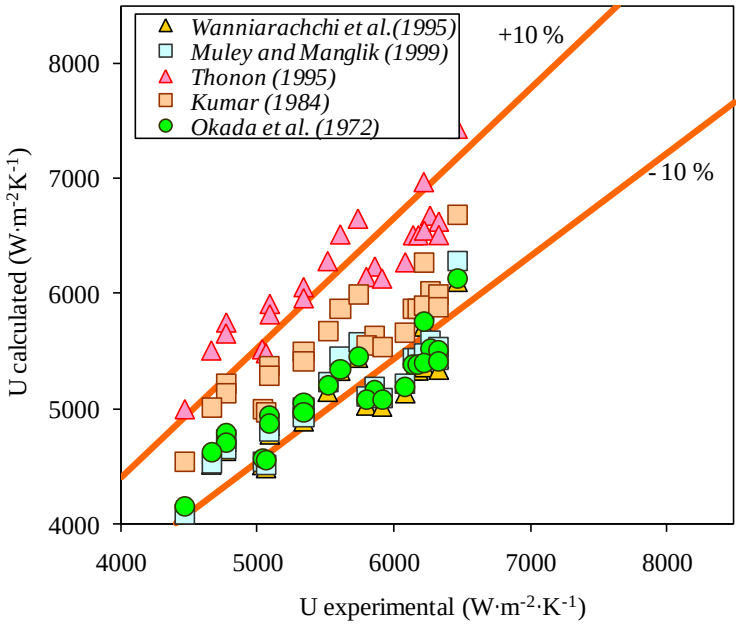

Figure 3. Differences between the calculated and experimental overall heat transfer coefficient, in single phase experiments with water obtained by available correlations

Figure 4

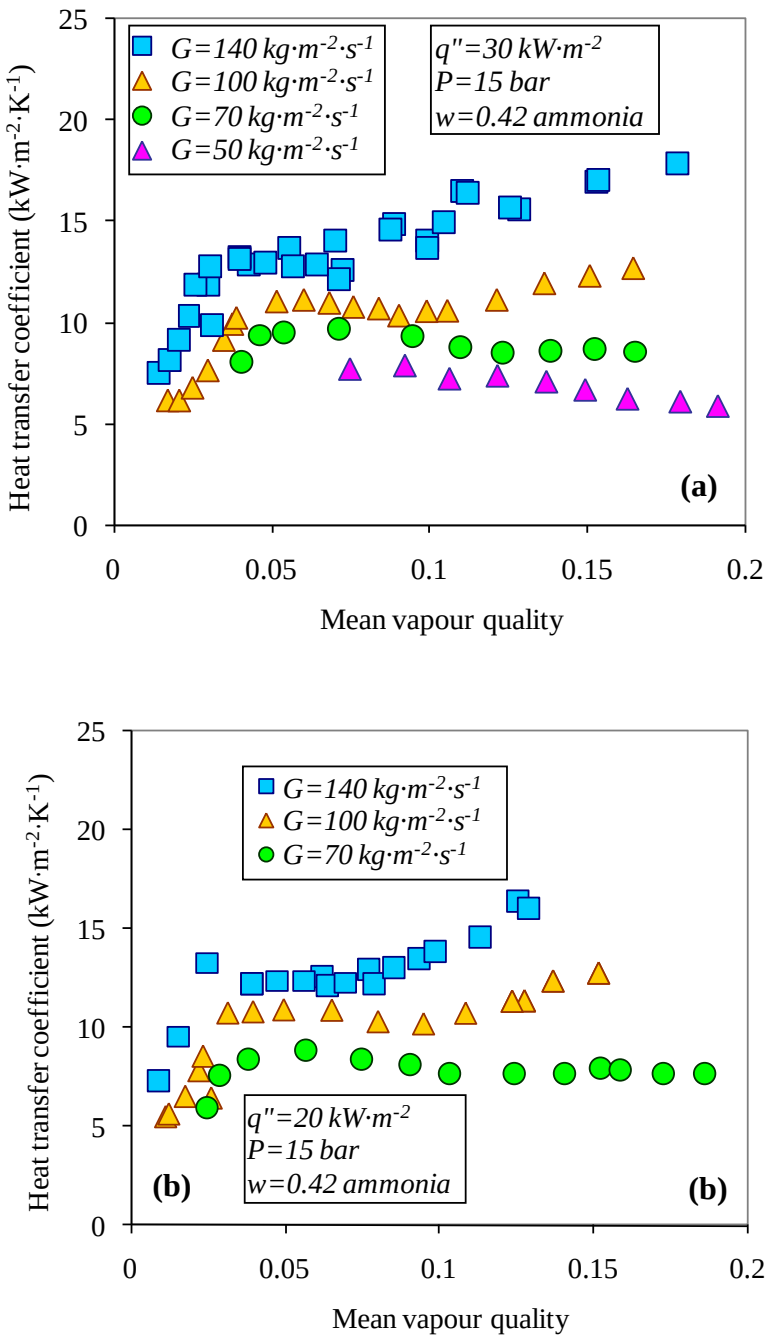
Heat transfer coefficient (kW·m-2·K-1)
Mean vapour quality
G=140 kg·m-2·s-1
G=100 kg·m-2·s-1
G=70 kg·m-2·s-1
G=50 kg·m-2·s-1
q"=30 kW·m-2
P=15 bar
w=0.42 ammonia
(a)
q"=20 kW·m-2
P=15 bar
w=0.42 ammonia
(b)
(b)

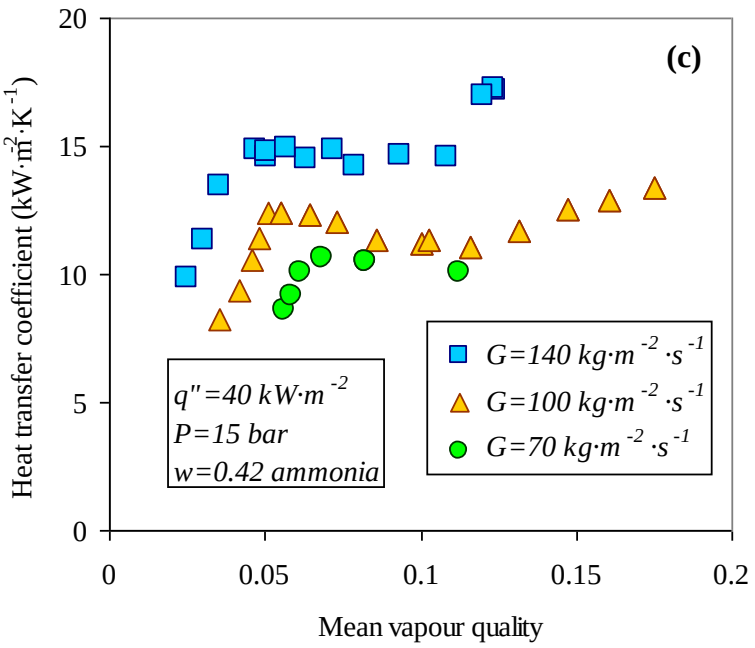

Figure 4. Boiling heat transfer coefficient vs. the mean vapour quality for different mass fluxes ((a): q"=30 kW·m^{-2}, P=15 bar, w=0.42 ; (b): q"=20 kW·m^{-2}, P=15 bar, w=0.42 ; (c): q"=40 kW·m^{-2}, P=15 bar, w=0.42)

Figure 5

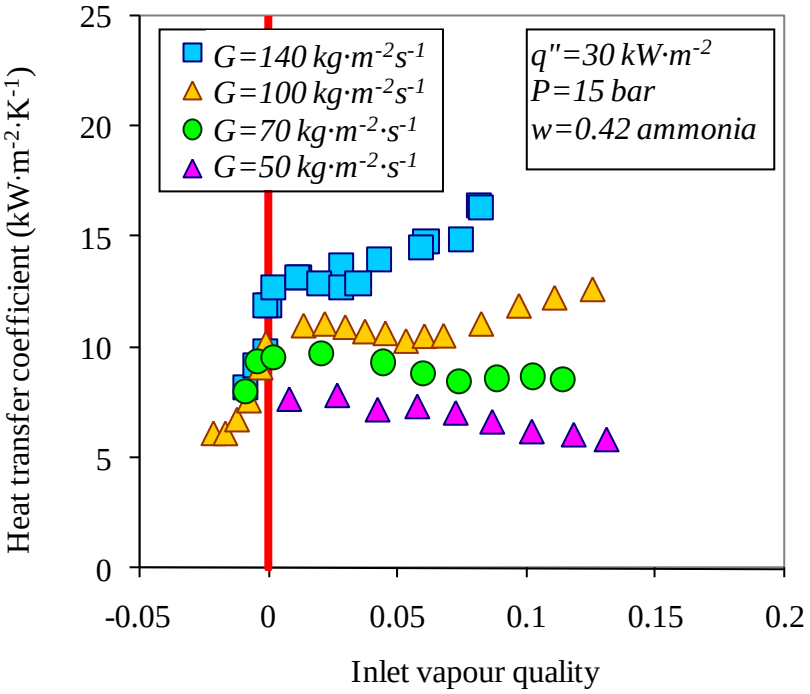

Figure 5. Boiling heat transfer coefficient vs.the inlet vapour quality for different mass fluxes (q"=30 kW·m^{-2}, P=15 bar, w=0. 42)

Figure 6

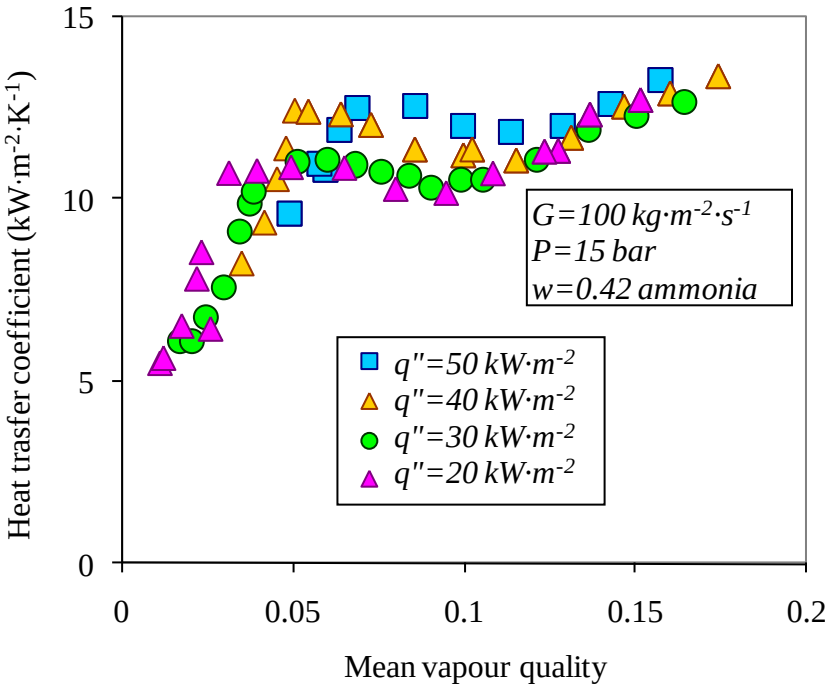

Figure 6. Boiling heat transfer coefficient vs. the mean vapour quality for different heat fluxes (G=100 kg·m^{-2}·s^{-1}, P=15 bar, w=0. 42)

Figure 7

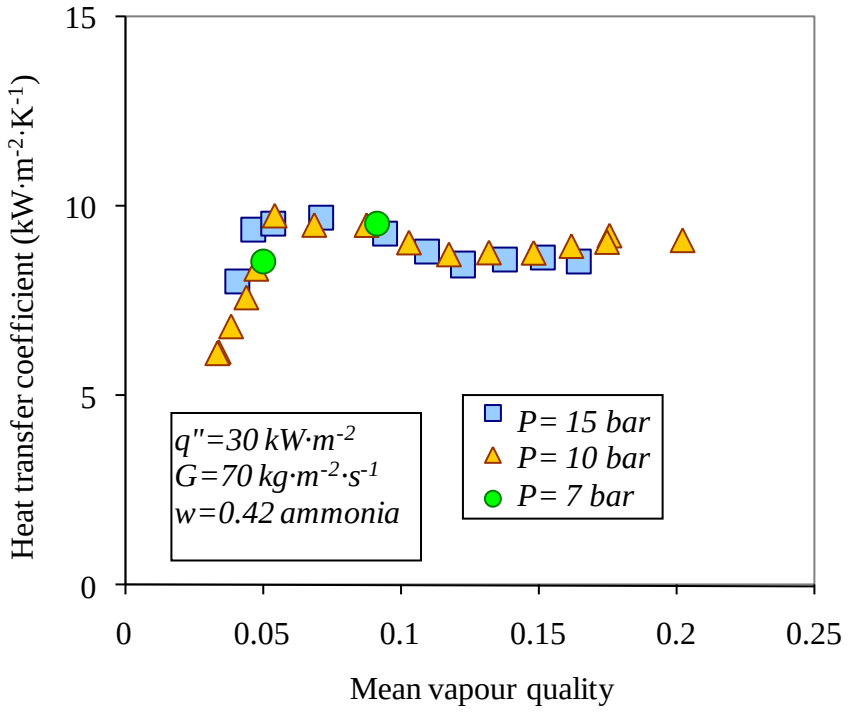

Figure 7. Boiling heat transfer coefficient vs. the mean vapour quality for different pressures (G=70 kg·m^{-2}·s^{-1}, q”=30 kW·m^{-2}, w=0. 42)

Figure 8

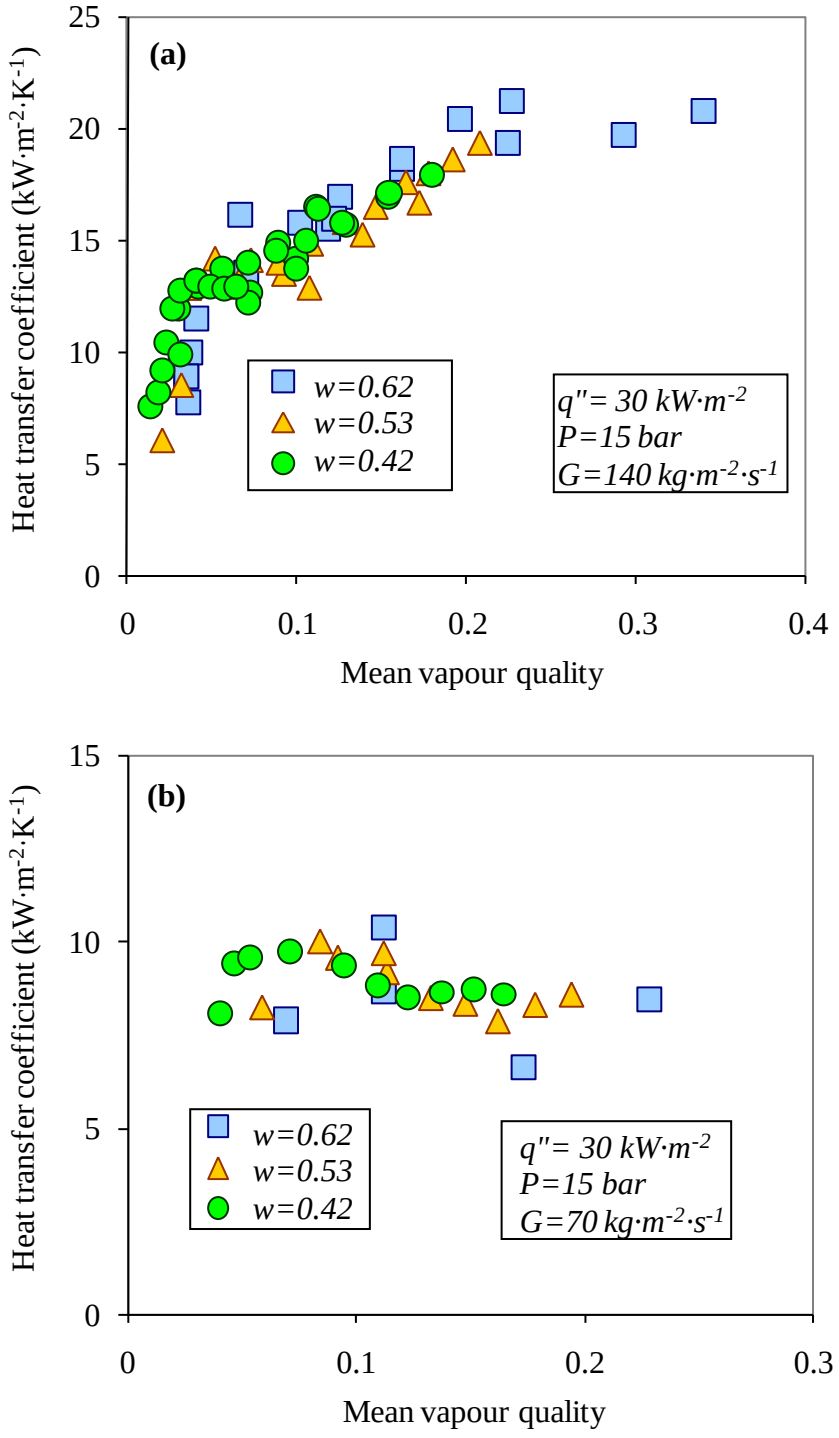

Figure 8. Boiling heat transfer coefficient vs. the mean vapour quality for different ammonia mass fractions (q"=30 kW·m^{-2}, P=15 bar, (a): G=140 kg·m^{-2}·s^{-1} and (b): G=70 kg·m^{-2}·s^{-1})

Figure 9

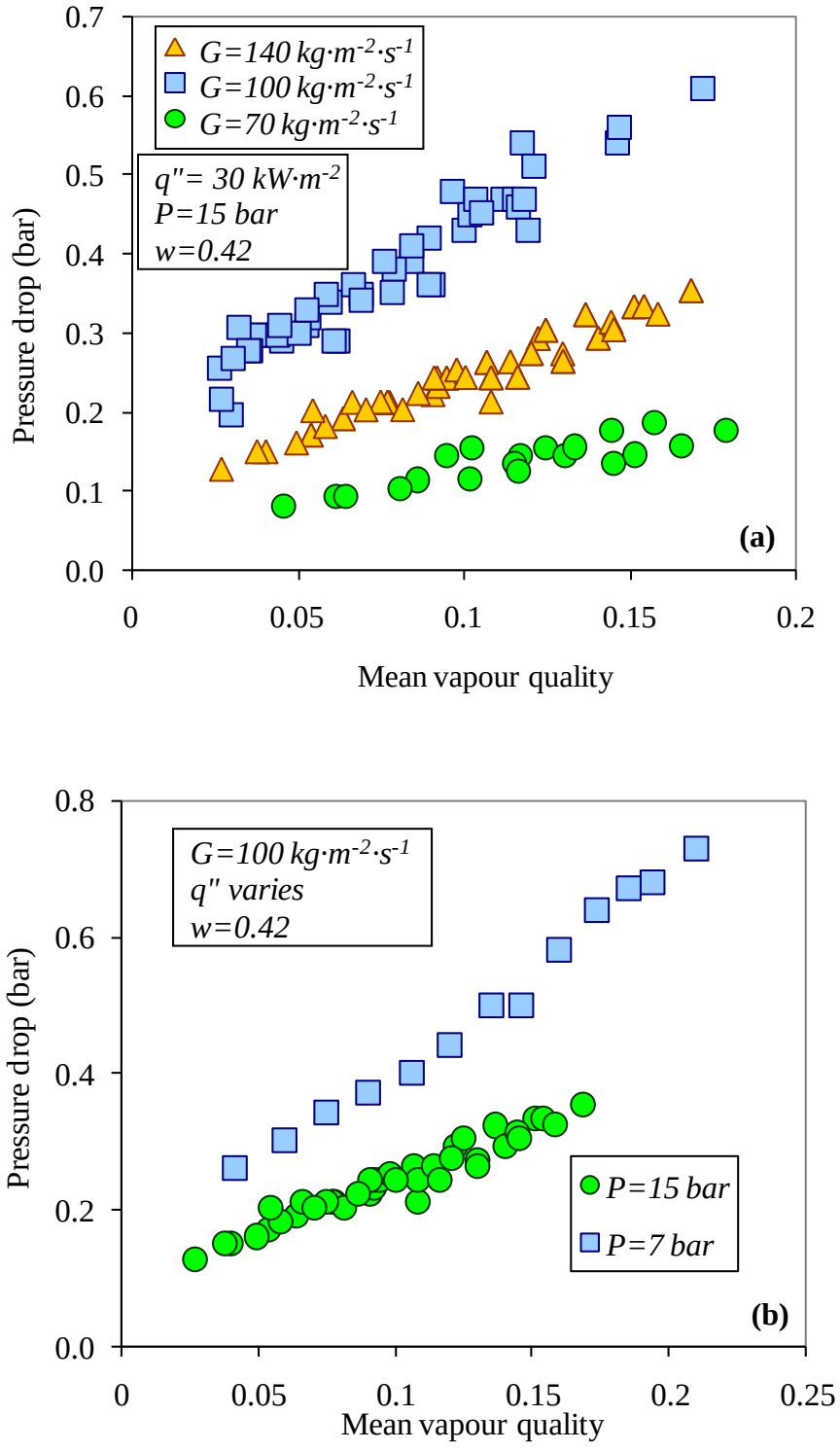

Figure 9. Pressure drop vs. the mean vapour quality ((a): mass flux effect, (b) pressure effect)

Figure 10

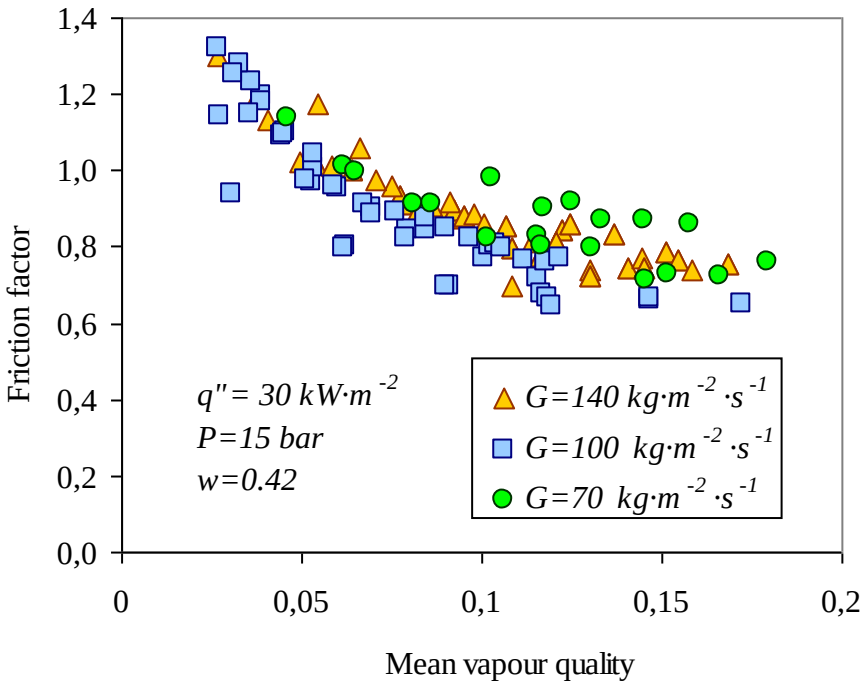

Figure 10. Friction factor vs. the mean vapour quality at different mass fluxes

Table 1

Table 1. Specifications of the plate heat exchanger

Surface area (m^2)	0.05
Length (m)	0.536
Width (m)	0.112
Cross section area (cm^2)	2
Plate separation (mm)	2
Plate thickness (mm)	0.4
Hydraulic diameter (mm)	4

Table 2

Table 2. Summary of the uncertainty analysis

Parameter	**Uncertainty**
Measurements	
Temperature, T (°C)	± 1
Pressure, P (Pa)	± 1600
Water flow rate, m_w (%)	± 0,25
Solution flow rate, m_s (%)	± 0.1
Solution concentration (%)	±1
Heat transfer	
Heat transfer rate, Q (%)	±1.7 - 4.5
Vapour quality, x (%)	±0.03 - 0.0134
Boiling heat transfer coefficient, h (%)	±5.6 - 16.4
Pressure drop	
Fanning friction factor (%)	±8-18.2